Available online at www.sciencedirect.com
SCIENCE DIRECT®
Materials and Design 25 (2004) 103–109
Materials & Design
www.elsevier.com/locate/matdes

Microstructure and properties of a laser fabricated burn-resistant Ti alloy

X. Wu [a,*], R. Sharman [a], J. Mei [a], W. Voice [b]

[a] IRC in Materials for High Performance Applications, The University of Birmingham, Edgbaston B15 2TT, UK
[b] Rolls-Royce plc. P.O. Box 31, Derby DE24 8BJ, UK

Received 7 April 2003; accepted 9 October 2003

Abstract

The response of a recently developed burn-resistant Ti alloy (Ti–25V–15Cr–2Al–0.2C, wt%) to direct laser fabrication has been assessed. The influence of laser processing conditions on the microstructure and on the tensile properties at room and at elevated temperatures and on the creep properties has been investigated. In contrast to Ti–6Al–4V the burn-resistant alloy has been found to form equiaxed, rather than columnar grains during laser fabrication for a very wide range of processing conditions. The factors which influence whether equiaxed grains or columnar grains are formed during laser fabrication are discussed and the influence of the laser process route on properties is discussed in terms of the microstructural differences found in laser fabricated and conventionally processed samples.

Keywords: Lasers; Non-ferrous metals and alloys; Microstructure; Mechanical properties

1. Introduction

Direct laser fabrication (or LENS) is a technique which can build up a 3-D component from a CAD file using powder which is ejected into a laser focal point [1–7] and a 3-D geometry is formed by building-up a stack of 2-D profiles layer by layer. This technique has a great potential for repairing components, for adding on small parts on big components or for manufacturing individual components simply from a CAD file without the need for tooling. Laser fabrication can be used to repair or to tip turbine or compressor blades rather than using TIG welding with the advantage that the heat affected zone will be much smaller using a laser rather than conventional welding.

Hence, the aim of the present work is to use laser fabrication to manufacture samples from a Ti alloy suitable for tipping blades. This alloy, a burn-resistant beta Ti alloy, (Ti–25V–15Cr–2Al–0.2C (wt%) [8–11]), has been developed with Rolls-Royce as a wrought alloy and the microstructure and properties of extruded products are well known. In order to use this alloy for blade tipping, it is necessary to understand its response to laser fabrication, not only in terms of the variables such as laser power, but also the influence on properties and microstructure of the different thermal histories in different locations in a component.

The properties and microstructure of laser fabricated Ti6Al4V have been investigated in earlier work [6] and it has been found that Ti64 tends to form columnar grains and that the microstructure is a sensitive function of the processing conditions and that different regions have different microstructures, which is undesirable for critical structural components. Some laser fabrication work has been carried on other Ti alloys, e.g., Ti–10V–2Fe–3V and Ti burn-resistant alloy [5,7], and it has been noted in preliminary studies that Ti burn-resistant alloy responds differently to laser fabrication from Ti6Al4V [7]. In this study, the effects of processing conditions on the microstructure of the burn-resistant alloy have been fully investigated and tensile, fatigue and creep properties of the laser deposited samples have been measured. The different response of the burn-resistant alloy to laser

* Corresponding author. Tel.: +44-121-414-7842; fax: +44-121-414-7890.
E-mail address: x.wu.1@bham.ac.uk (X. Wu).

0261-3069/$ - see front matter © 2003 Elsevier Ltd. All rights reserved.
doi:10.1016/j.matdes.2003.10.004

fabrication with respect to the Ti6Al4V is discussed in terms of the differences in their phase diagrams.

2. Experimental

The ingot of the burn-resistant alloy Ti–25V–15Cr–2Al–0.2C (wt%) was produced in the plasma melter in the IRC and was gas atomised by Crucible, Pittsburgh, USA. The oxygen content in the atomised powder was ~1900 ppm (0.19 wt%). The Ti–6Al–4V (wt%) substrate, onto which the laser product was deposited, was part of a rolled plate with a thickness of 30 mm. The laser-built specimens were produced using a 1.75 kW CO_2 laser in an argon atmosphere with $O_2 < 5$ ppm. The laser fabrication parameters used in this study are shown in Table 1 where the *Z*-increment is the step height between successive layers. In this work, 1–1.5 mm thick rectangular samples and rods with a length of 80 mm and a diameter of 20 mm were produced.

A Philips XL30 SEM, fitted with EDX and EBSD systems, was used to examine the microstructure of the samples. An optical microscope was also used to assess the homogeneity of the microstructure of the entire build. The volume fraction of the precipitates was measured by using image analysis.

Table 1
Showing the parameters used for deposition of Ti–25V–15Cr–2Al–0.2C (wt%)

Processing parameters	
Laser power (W)	222, 264, 306, 348, 390, 432, 474, 516
Powder size (μm)	100–250
Powder feed rate (g/min)	9, 12, 18, 24
Laser scanning rate (mm/min)	200, 300, 400, 500, 600, 700, 800
Z-increment (mm)	0.25, 0.35

Some of the laser fabricated rods were HIPped (Hot Isostatically Pressed) at 1000 °C/100 MPa for 4 h before being machined. Tensile tests were carried out at room temperature and at 450 °C and creep tests were conducted at temperatures of 450, 550 and 650 °C at stresses of 650, 300, 200 MPa, respectively.

3. Results

The microstructures of the laser fabricated Ti burn-resistant alloy obtained at various laser powers are shown in Figs. 1 and 2. It should be noted that all micrographs shown in this paper are longitudinal sections. In general this alloy tends to form equiaxed grains under most laser processing conditions, although a few elongated grains have been observed at the bottom of samples at some laser powers such as 348 and 390 W (Fig. 1(d) and (e)) and the height of this region is normally less than 1 mm (i.e., about 3–4 *Z*-increments), which is significantly shorter than that seen in Ti64 in which columnar grains were normally formed throughout entire samples [6]. Fig. 2 shows the microstructure which is formed throughout most of the sample fabricated within a range of laser powers. It can be seen that equiaxed grains of beta phase dominate in these microstructures and precipitates are uniformly distributed within the beta grains and at the grain boundaries. With increase of laser power from 222 to 516 W limited grain growth was observed in beta grains, however the volume fraction of the precipitates was increased with increase of the laser power (Fig. 3). The volume fraction of the precipitates is approximately 16% in the top region of the sample for the laser power of 516 W. This is much more than the equilibrium volume fraction of Ti_2C carbides, which is approximately 4% according to the calculation based on the 0.2 wt% C content.

Fig. 4 shows the effects of laser scan speed on the morphology of the laser build. It is clear that for a given

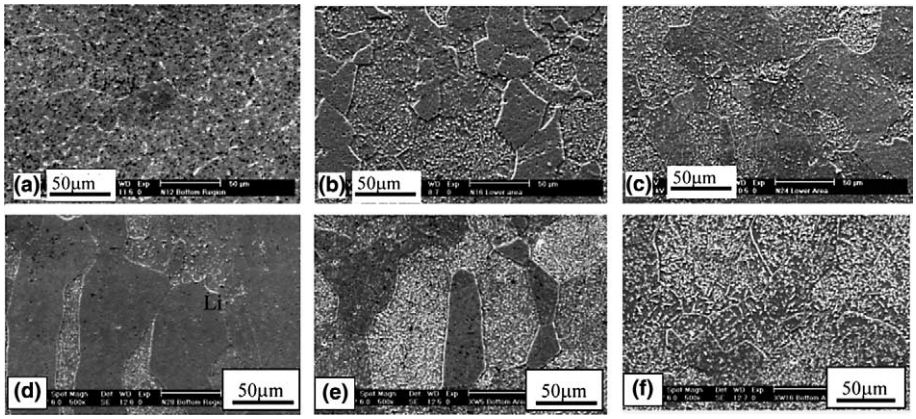

Fig. 1. Secondary SEM micrographs showing the morphologies at the bottom of BurTi samples laser-deposited at a scan speed of 200 mm/min, powder feed rate of 9 g/min and at a range of laser powers: (a) 222; (b) 264; (c) 306; (d) 348; (e) 390 and (f) 516 W.

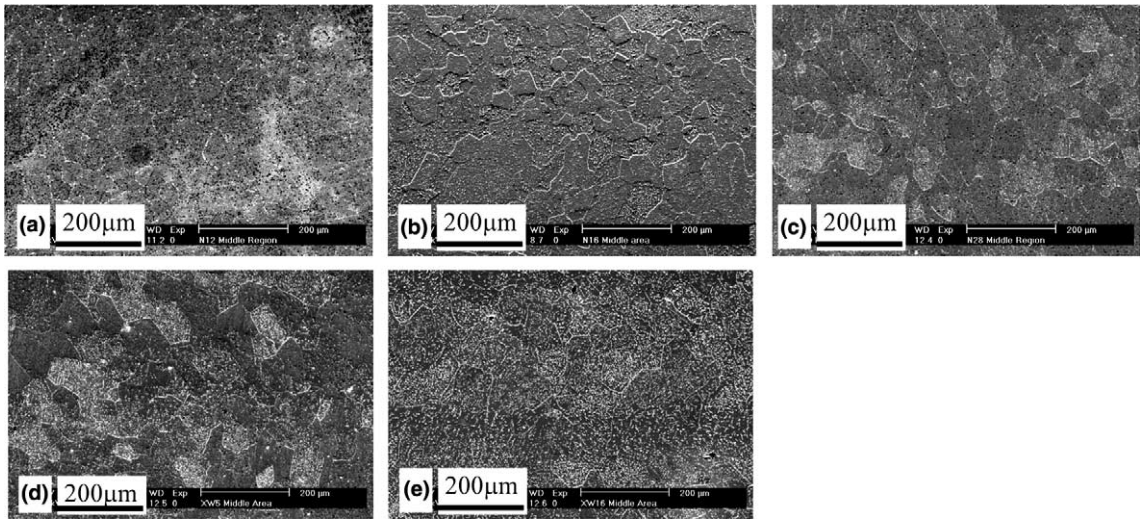

Fig. 2. Secondary SEM micrographs showing equiaxed grains at the centre (and top) of BurTi samples laser-deposited at a scan speed of 200 mm/min, powder feed rate of 9 g/min and at a range of laser powers: (a) 222; (b) 264; (c) 348; (d) 390 and (e) 516 W.

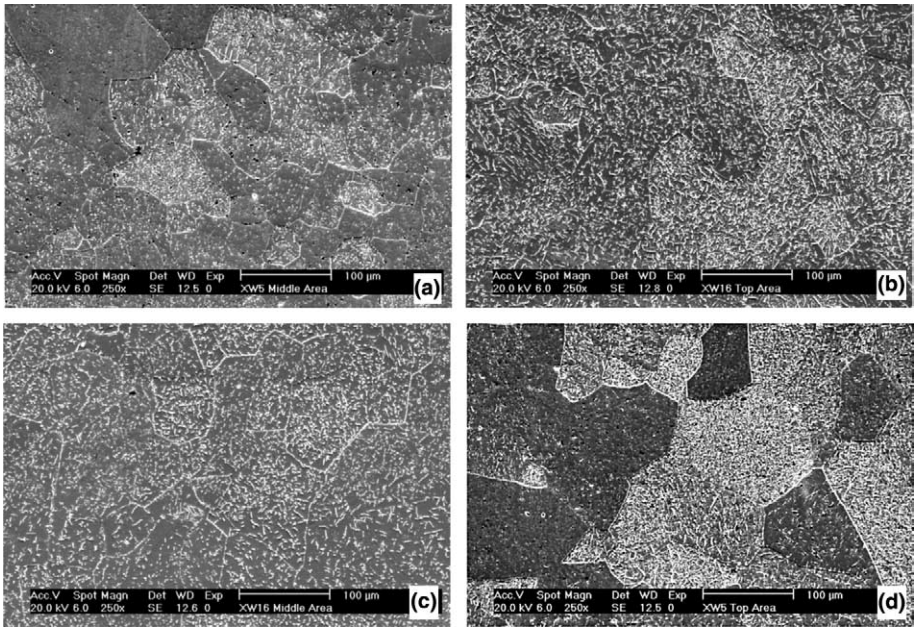

Fig. 3. Secondary SEM micrographs showing the change of volume fraction of precipitates with the location in the sample and the laser power: (a, b) 390 and (c, d) 516 W. (a, c) at the centre and (b, d) at the top of samples. The laser scan speed was 200 mm/min and powder feed rate was 9 g/min.

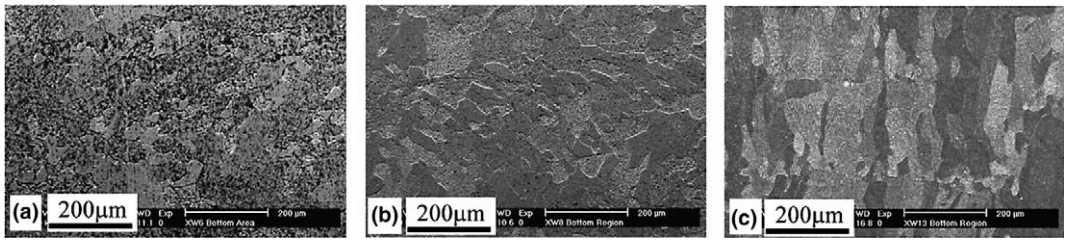

Fig. 4. Secondary SEM micrographs showing the influence of scan speed on the morphology at the bottom of DLFed BurTi at a powder feed rate of 18 g/min and a laser power of 390 W: (a) 200 mm/min, height (h) = 21.2 mm; (b) 400 mm/min, h = 22.5 mm and (c) 1050 mm/min, h = 5.2 mm. The height (h) is the actual height of the build obtained for a defined height of 20 mm which has been input into the computer programme.

laser power and powder feed rate, an increase of scan speed enhances formation of columnar grains in the microstructure. It is also noted that at a very high scan speed samples cannot be built beyond some small height at a fixed powder feed rate. For example at a scan speed of 1050 mm/min for a defined sample height of 20 mm and Z-increment of 0.3 mm, the actual height obtained is only 5.2 mm. The influence of scan speed was observed to become more distinctive with decrease of powder feed rate. At a powder feed rate of 9 g/min, columnar grains were formed now at 400 mm/min (Fig. 5). At 1050 mm/min, the actual height of the sample obtained was only approximately 2 mm.

Fig. 6 shows the influence of scan speed on precipitation for a given powder feed rate of 18 g/min. It appears that with increase of scan speed precipitates become finer. However, this deduction may not be true in the case of low powder feed rates since samples with a limited height (e.g., only 2 mm high build is obtained at a powder feed rate of 9 g/min) were repeatedly scanned and it is likely that such repeated scanning would promote precipitate growth.

The effects of powder feed rate on the morphology, at the bottom and at the centre of the DLFed BurTi are shown in Fig. 7. For a given scan speed of 400 mm/min and laser power of 390 W, the height of samples obtained varies with powder feed rate even when the input height is the same. At a low powder feed rate of 9 g/min, only 13 mm is obtained for 20 mm input. The full height is achieved for the other two powder feed rates used, 18 and 36 g/min. It is also noted that a lower powder feed rate leads to formation of columnar grains at the bottom of the sample, Fig. 7(a). However, in the middle and the top of the samples powder feed rates have little effect on the microstructure and the precipitates.

Some of the DLFed rods were HIPped at 1000 °C/100 MPa/4 h. The HIPped microstructure is shown in Fig. 8(a). In comparison to the microstructure prior to

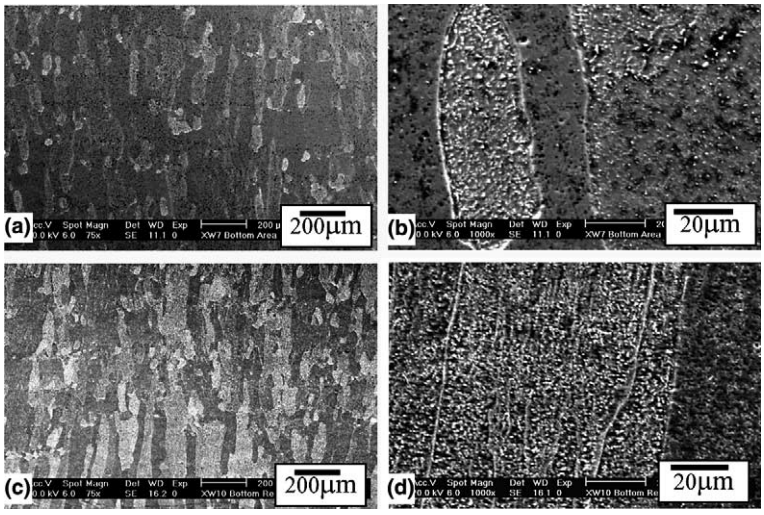

Fig. 5. Secondary SEM micrographs showing that columnar grains were formed at a lower scan speed of 400 mm/min at the bottom of the sample when the powder feed rate is reduced to 9 g/min (compare with Fig. 4): (a, b) 400 mm/min, height (h) = 12.8 mm and (c, d) 800 mm/min, h = 2 mm. The laser power was 390 W.

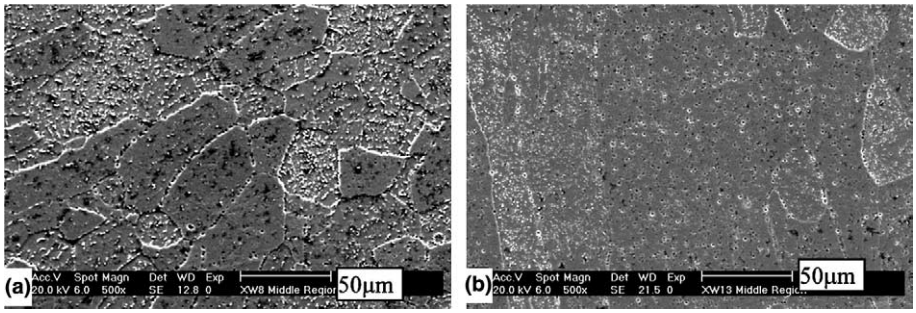

Fig. 6. Secondary SEM micrographs showing the effect of the scan speed on precipitation for a given powder feed rate of 18 g/min and laser power of 390 W: (a) 400 mm/min and (b) 1050 mm/min.

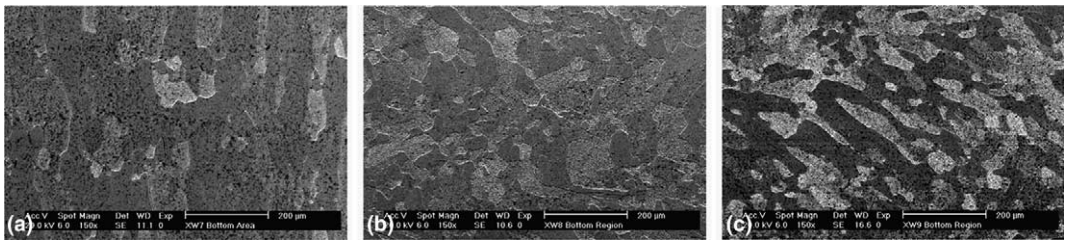

Fig. 7. Secondary SEM micrographs showing the influence of powder feed rates on the morphology at the bottom of DLFed BurTi at a scan speed of 400 mm/min and a laser power of 390 W: (a) 9 g/min, height (h) = 13 mm; (b) 18 g/min, h = 20 mm and (c) 36 g/min, h = 20 mm. The height (h) is the actual height of the build obtained for a defined height of 20 mm which was input into the computer programme.

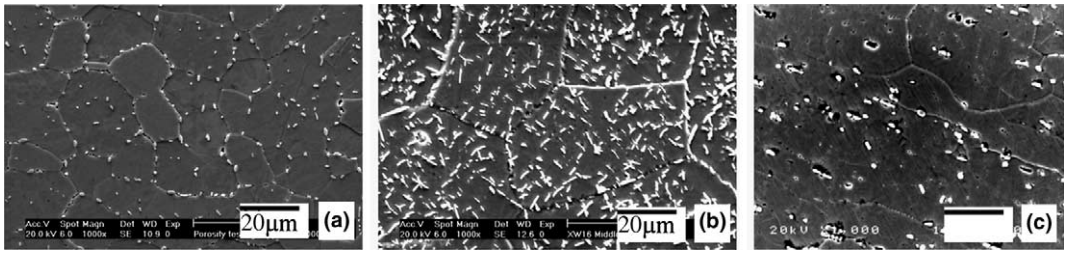

Fig. 8. Secondary SEM micrographs showing a comparison of microstructures obtained after: (a) DLFed + HIPped, (b) DLFed and (c) conventional microstructure obtained after forging.

HIPping (Fig. 8(b)), the difference in the volume fraction of the precipitates before and after HIPping is apparent. The volume fraction of the precipitates has been reduced from approximately 16% in the as-DLFed microstructure to 4% after subsequent HIPping. Fig. 8(c) shows the microstructure obtained via conventional process route of forging, where the volume fraction of the carbides is approximately 4%, corresponding to the Ti_2C (or Ti(CO)) volume fraction calculated according to the C content in the material. It is also noted that the size of β grains and precipitates is finer after HIPping with respect to the as-DLFed microstructure (compare Fig. 8(a) with Fig. 8(b)) and the precipitates are located mostly at the β grain boundaries (Fig. 8(a)).

Some tensile, fatigue and creep tests have been carried out on HIPped samples and for comparison samples which were cast as ingots and extruded have also been tested. Some of the results are shown in Figs. 9–11. Fig. 9 shows the tensile properties at room temperature for DLFed + HIPped and as-DLFed microstructures and at 450 °C for HIPped microstructure. The ductility of the HIPped samples is 2–4% at room temperature and at 450 °C, which is similar to that obtained normally in the extruded microstructure for a same oxygen level (1900 ppm). Note that the un-HIPped samples failed in the elastic regime. Further work is being carried out comparing the mechanical properties between DLFed + HIPped and as-DLFed for a range of laser processing conditions.

The fatigue properties (see Fig. 10) of the DLFed + HIPped condition have been found to be comparable to the extruded condition at all the conditions tested, i.e., 650 MPa/450 °C, 300 MPa/550 °C and 200 MPa/650 °C. Note that the creep properties of the HIPped microstructure are far better than those of extruded condition for the range of loads and temperatures investigated although the β grain size in the HIPped condition is much smaller (Fig. 11).

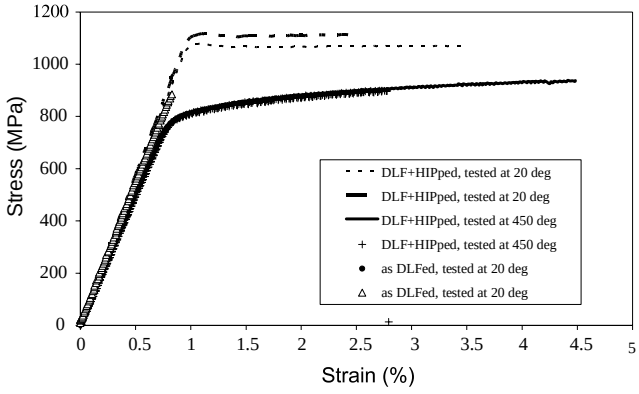

Fig. 9. Stress-strain curves of the burn-resistant alloy obtained under tensile loading at room temperature and 450 °C for as-DLFed and DLF + HIPped samples. Showing that DLF + HIPped samples have 2–4% ductility which is similar to that in extruded bulk samples for the same oxygen level and also showing that as-DLFed samples (without HIPping) failed prior to any plastic deformation.

4. Discussion

The results have shown firstly that the influence of laser processing parameters on the microstructure is small. The

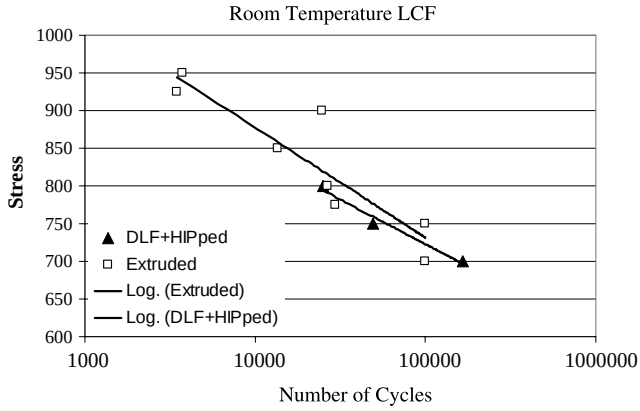

Fig. 10. A comparison of fatigue behaviour between DLF + HIPped microstructure and extruded microstructure of the burn-resistant alloy and showing that low cycle fatigue properties are comparable.

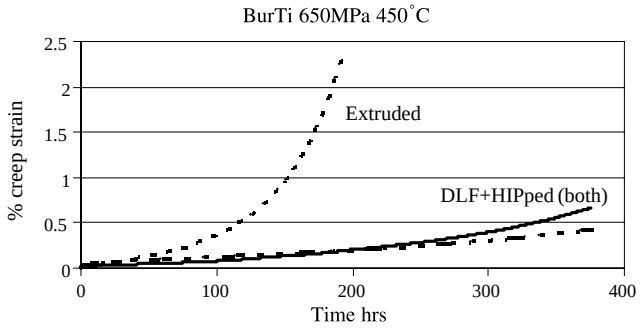

Fig. 11. A comparison of creep properties of the burn-resistant alloy between the extruded microstructure and DLF + HIPped microstructure tested at 650 MPa and at 450 °C. Tests of DLF + HIPped samples were interrupted after 380 h without failure of the samples. DLF + HIPped samples have superior creep resistance.

overall microstructure obtained in this alloy is dominated by equiaxed grains for a large range of process conditions. Some elongated grains about 1–2 mm in length have been seen at some process conditions which are far smaller than those found in Ti–6Al–4V where columnar grains dominate entire samples under most conditions. Secondly, the volume fraction of precipitates in the DLFed microstructure of the burn-resistant alloy can be as high as 16% for some processing conditions, which is much more than the amount of equilibrium carbide present in the material. Finally, the mechanical properties of the DLFed + HIPped microstructure are comparable to, if not better than those in extruded samples. In the case of creep, the DLFed + HIPed microstructure has superior properties despite the smaller β grain size. These results will be discussed in turn.

The formation of equiaxed or columnar grains during solidification is normally influenced by the extent of directional cooling, by the presence of externally added nuclei and by the gap and slope of the liquidus–solidus. For a given size of substrate and a given laser condition, the temperature gradient from the build to the substrate

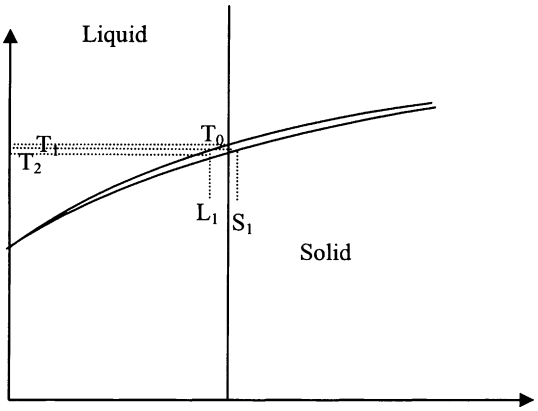

Fig. 12. A schematic illustration showing liquidus and solidus and the solidification sequence in the burn-resistant alloy. T_0 is the liquidus for the alloy considered; T_1 is the temperature when nucleation is assumed to occur; $(T_0–T_1)$ is then the under-cooling. T_2 is the assumed nucleation temperature for the liquid of composition L_1.

and to the surrounding areas will be similar between different Ti alloys. Potential nuclei can be added to a molten pool since some large powder particles may not fully melt and they can serve as nuclei and promote the formation of equiaxed grains. It would be expected that the role of these potential nuclei would be similar for different alloys. The fact that the burn-resistant alloy and Ti64 behave so differently in terms of formation of equiaxed grains must then be associated with intrinsic differences in the solidification behaviour, which in turn is influenced by the nature of the phase diagram. A schematic illustration of the Ti–V phase diagram which is taken to represent Ti–25V–15Cr–2Al is shown in Fig. 12. It can be seen that the liquidus–solidus gap in Ti–V phase diagram is very small and the slope is also very small in comparison to Ti–Al phase diagram for alloy Ti64 [12]. Thus, when nucleation of a solid grain occurs in a Ti–V based system, the compositional difference between the liquid and solid will be small. The temperature at which further solidification will occur in this alloy is thus not reduced to the same extent as is the case for Ti64 where the slope and separation of the liquidus–solidus are larger. Hence, nucleation of new grains is likely for modest temperature gradients in the burn-resistant alloy. The influence of process variables on the propensity to form columnar or equiaxed grains can thus be understood. With increase of laser scan speed a build undergoes rapidly repeated heating and the liquid in a molten pool remains hot and newly solidified fine grains on top of the build may also be remelted, which will suppress the nucleation from the liquid and enhance the formation of columnar grains, as shown in Figs. 4 and 5. The influence of the powder feed rate can also be associated with the same mechanism because the liquid in a molten pool would be hotter for low powder feed rates when the same laser energy and the probability of nucleating new grains reduced (Fig. 4).

Figs. 1, 5 and 8(b) have shown that the volume fraction of precipitates in DLFed microstructure can be as high as 16%, which is four times higher than the volume fraction expected in the material under equilibrium conditions. The amount of precipitates was reduced to about 4% during HIPping (compare Fig. 8(a) with Fig. 8(b)). This indicates that the precipitates in the DLFed microstructure are a non-equilibrium phase or a low temperature phase formed during reheating which occurs during DLF and they are transformed during HIPping. The equilibrium carbide phase in the material is $Ti(C_xO_y)$ [8], which for 0.2 wt% carbon content would give about 4 vol% of precipitate since analysis shows that the oxygen content remained at about 1900 ppm during laser fabrication. Detailed TEM work is currently underway to identify the nature of these precipitates in the DLFed samples.

The strength and ductility of the burn-resistant alloy are controlled by the oxygen level and the β grain size. The fatigue properties of the material are markedly affected by the size of carbides and by the ductility of the matrix material. The size of precipitates in the DLFed + HIPped microstructure is about 2 μm, slightly smaller than the size in the extruded microstructure. The improvement in the tensile and fatigue properties of the DLFed microstructure is thus expected. On the contrary, because the β grain size is much smaller (compare Fig. 8(a) with Fig. 8(b) and (c)), the creep resistance would be expected to be reduced. However, Fig. 8(a) shows that the majority of precipitates were located at the grain boundaries, whereas in the conventionally processed microstructure they are uniformly distributed throughout the grains. If the creep testing condition is in the range where creep is dominated by grain boundary sliding, the precipitates at the grain boundaries can pin the grain boundaries and lead to superior creep resistance, as shown in Fig. 11.

The present work has shown that the microstructure and mechanical properties of a material obtained using direct laser fabrication technique are not only influenced by processing conditions, but also by the solidification characteristics of the alloys. In order to produce a component with uniform microstructure and optimum mechanical properties it is important to select a material, which has propensity to form a microstructure of equiaxed rather than columnar grains.

It has been found that the C forms a fine distribution of carbide precipitates which pin grain boundaries and thus limit grain growth. In addition, the Ti_2C particles act as getters and remove oxygen from the matrix forming Ti(CO). This removal of oxygen not only improves the ductility of the forged and heat treated alloy, but also reduces the tendency for precipitation of alpha during high temperature exposure, leading to an increase in ductility over that found in exposed non carbon-containing alloy.

5. Conclusions

1. The burn-resistant alloy tends to form equiaxed grains rather than columnar grains during direct laser fabrication.
2. The microstructure of the burn-resistant alloy is relatively insensitive to the laser processing parameters.
3. The mechanical properties of the DLFed microstructure, followed by HIPping are equivalent, if not superior, to those obtained in extruded microstructure.

Acknowledgements

One of the authors, R Sharman, is a CASE student sponsored by Rolls-Royce plc, The University of Birmingham and EPSRC, Timet UK and MOD and DTI(CARAD). Thanks are due to Prof. M.H. Loretto for useful discussions.

References

[1] Keicher DM, Miller WD, Smugeresky JE, Romero JA. Laser Engineered Net Shaping (LENS + TMS); Beyond rapid prototyping to direct fabrication. TMS Annual Meeting, 1998, p. 369–77.
[2] Atwood C, Griffith M, Harwell L, Schlienger E, Ensz M, Smugereskey JE, Romero T, Greene D, Reckaway D. Laser engineered net shaping (LENS): a tool for direct fabrication of metal parts. In: Proceedings of the International Congress on Applications of Lasers and Electro-Optics (ICALEO '98). Laser Institute of America, vol. E, 1998, p. 1–7.
[3] Lewis GK, Schlienger E. Practical considerations and capabilities for laser assisted direct metal deposition. Mater Design 2000;21:417–23.
[4] Griffith ML. Understanding thermal behaviour in the LENS process. Mater Design 1999;20:107–13.
[5] Wu X, Sharman R, Mei J, Voice W. Direct laser fabrication and microstructure of a burn-resistant Ti alloy. Mater Design 2002;23:239–47.
[6] Goodwin P S, Mitchell C, Liang J, Mei J, Wu X. The Influence of processing parameters on the formation of pores and columnar grains in laser deposited Ti–6Al–4V alloy, 2002. In: International Conference on Metal Deposition for Rapid Manufacturing, April 8–10, 2002, San Antonio, Texas.
[7] Wu X, Mei J, Sharman R, Voice W. Microstructure and mechanical properties of a laser fabricated Ti alloy, 2002. In: International Conference on Metal Deposition for Rapid Manufacturing, April 8–10, 2002, San Antonio, Texas.
[8] Li YG, Blenkinsop PA, Loretto MH, Rugg D, Voice W. Acta Mater 1999;47(10):2889–905.
[9] Li YG, Blenkinsop PA, Loretto MH, Walker N. Acta Mater 1998;46(16):5777–94.
[10] Li YG, Blenkinsop PA, Loretto MH, Walker N. Mater Sci Tech 1998;14:732–7.
[11] Li YG, Blenkinsop PA, Loretto MH, Walker N. Mater Sci Tech 1999;15:151–5.
[12] Mitchell A, Tripp D. Solidification and segregation in titanium alloys. In: 1986 International Conference on Titanium Products and Applications. p. 1011–9.